Running of the heavy quark production current and 1/|k| potential in QCD

Aneesh V. Manohar* and Iain W. Stewart†

Department of Physics, University of California at San Diego, 9500 Gilman Drive, La Jolla, California 92093

The 1/$\mathbf{k}$ contribution to the heavy quark potential is first generated at one loop order in QCD. We compute the two loop anomalous dimension for this potential, and find that the renormalization group running is significant. The next-to-leading-log coefficient for the heavy quark production current near threshold is determined. The velocity renormalization group result reproduces the $\alpha_s^3 \ln^2(\alpha_s)$ ''nonrenormalization group logarithms'' of Kniehl and Penin.

I. INTRODUCTION

For systems involving a heavy-quark–antiquark pair near threshold it is useful to combine the QCD coupling constant expansion with an expansion in powers of the relative velocity v. This expansion is facilitated by using nonrelativistic QCD (NRQCD) formulated as an effective field theory with an explicit power counting in v [1–14]. For the potential between a heavy quark and antiquark this double expansion takes the form

$$V(\mathbf{p},\mathbf{p}') = \sum_{n=-2}^{\infty} V^{(n)}, \quad V^{(n)} = \sum_{j=1}^{\infty} V^{(n,j)},$$

$$\text{where} \quad V^{(n)} \sim v^n, \quad V^{(n,j)} \sim v^n \alpha_s^j. \quad (1)$$

The even terms $V^{(2k)}$ are first generated at tree level (order α_s), and the odd terms $V^{(2k+1)}$ are first generated at one loop (order α_s^2).

Matrix elements for nonrelativistic QCD systems typically depend on logarithms of the velocity v. For small v it is convenient to sum large logarithms of the form $\alpha_s(mv)\ln(v)$ and $\alpha_s(mv^2)\ln(v)$ by using renormalization group equations in the effective theory. This reorganizes the series in j in Eq. (1) so that

$$V^{(n)} = \sum_j \widetilde{V}^{(n,j)},$$

$$\text{where} \quad \widetilde{V}^{(n,j)} \sim v^n \alpha_s(m)^j \sum_{k=0}^{\infty} [\alpha_s(m)\ln(v)]^k. \quad (2)$$

The simplest example of such a summation is the use of a running coupling constant, $\alpha_s(\mu)$, instead of the coupling at the matching scale $\alpha_s(m)$. For $\mu < m$ the running coupling includes a series of $\alpha_s(m)\ln(\mu/m)$ terms. However, it should be emphasized that the complete set of renormalization group logarithms are not determined by the simple replacement $\alpha_s(m) \rightarrow \alpha_s(\mu)$.

A complication in summing the logarithms is the presence of two low energy scales: the typical momenta of the heavy quark $\sim mv$ (soft scale), and typical energy $\sim mv^2$ (ultrasoft

scale). Two approaches have been proposed for dealing with the presence of two scales, one stage and two stage running. With two stage running, one matches QCD onto an effective theory at the scale $\mu = m$ and then runs to the scale $\mu = mv$. At $\mu = mv$ one matches onto an effective theory called potential NRQCD (pNRQCD) [8,15] which has composite $q\bar{q}$ fields, and then considers the running to $\mu = mv^2$. In vNRQCD [14], the running occurs in a single stage using a velocity renormalization group. The velocity renormalization group takes into account that the scales mv and mv^2 are tied together by the heavy quark equation of motion for all $\mu < m$. We use dimensional regularization and the modified minimal subtraction ($\overline{\text{MS}}$) scheme with both the ultrasoft scale $\mu_U \sim mv^2$ and the soft scale $\mu_S \sim mv$ given in terms of a single subtraction point velocity ν: $\mu_U = m\nu^2$ and $\mu_S = m\nu$. The renormalization group equations are written for the variable ν. It is an interesting question as to whether both the one and two stage methods of running will sum the full set of $\alpha_s \ln(v)$ terms. In this paper only the single stage running will be considered.

The running of the Coulomb potential at one and two loops, $\widetilde{V}^{(-2,1)}$ and $\widetilde{V}^{(-2,2)}$, is determined by the running coupling constant $\alpha_s(\mu)$ [16].[1] The summation of the leading logarithms for the the v^0 potential was carried out in Refs. [18,19]. In this paper we extend this analysis to the 1/$\mathbf{k}$ potential by calculating its two loop anomalous dimension.

If $mv^2 \gg \Lambda_{\text{QCD}}$, the v expansion can be applied to nonrelativistic QCD systems in a perturbative manner. This is the case for $t\bar{t}$ production near threshold where $mv^2 \sim 4$ GeV, and is the situation that will be analyzed in this paper. Of particular interest is the Coulombic regime where $v \sim \alpha_s$. In this regime the expansion in Eq. (1) has the form

$$V = [\widetilde{V}^{(-2,1)}] + [\widetilde{V}^{(-2,2)}] + [\widetilde{V}^{(-2,3)} + \widetilde{V}^{(-1,2)} + \widetilde{V}^{(0,1)}] + \cdots$$

$$\sim \left[\frac{\alpha_s}{v^2}\right] + \left[\frac{\alpha_s^2}{v^2}\right] + \left[\frac{\alpha_s^3}{v^2} + \frac{\alpha_s^2}{v} + \alpha_s v^0\right] + \cdots. \quad (3)$$

If the $\alpha_s \ln(v)$ dependence is treated perturbatively these terms are referred to as the leading order (LO), next-to-

---

*Email address: amanohar@ucsd.edu
†Email address: iain@schwinger.ucsd.edu

---

[1]At three loops ultrasoft gluons can contribute to the running of the static potential [17].

leading order (NLO), and next-to-next-to-leading order (NNLO) potentials. Note that since the $1/|\mathbf{k}|$ potential first occurs at one loop, it only contributes at NNLO. When the series in $\alpha_s \ln v$ are summed, the terms in Eq. (3) will be referred to as leading-log (LL), next-to-leading log (NLL) and next-to-next-to-leading log (NNLL), respectively. In the Coulomb regime, the Coulomb potential must be kept to all orders. Each additional Coulomb insertion gives a α_s/v^2 plus a factor of v (from the potential loop), so each new Coulomb interaction costs a factor of $\alpha_s/v \sim 1$.

To study the threshold production of $t\bar{t}$, a nonrelativistic expansion must also be made for the electromagnetic production current[2]

$$\bar{t}\gamma^i t = \sum_{\mathbf{p}} c_1 (\psi_{\mathbf{p}}^\dagger \boldsymbol{\sigma}^i \chi_{-\mathbf{p}}^*) - \frac{c_2}{2m^2} (\psi_{\mathbf{p}}^\dagger \mathbf{p} \cdot \boldsymbol{\sigma} \, \mathbf{p}^i \chi_{-\mathbf{p}}^*)$$
$$- \frac{c_3}{m^2} (\psi_{\mathbf{p}}^\dagger \mathbf{p}^2 \boldsymbol{\sigma}^i \chi_{-\mathbf{p}}^*) + \cdots . \quad (4)$$

The fields ψ^* and χ^* create nonrelativistic top quarks and antiquarks, respectively. The c_1 term contributes at order v^0, and the c_2 and c_3 terms contribute at order v^2. The current on the left-hand side of Eq. (4) is conserved, and has no anomalous dimension in QCD. However, the nonrelativistic current operators on the right-hand side are scale dependent in the effective theory, and the coefficients c_j therefore depend on logarithms of μ. The coefficients c_j each have an expansion in α_s. The matching at $\mu \sim m$ is known to order α_s^2 for c_1 [20,21], and to order α_s for c_2 and c_3 [7], so the production current is known to NNLO with partial N^{3}LO results. At LL order, one needs the tree-level matching $c_1 = 1$ at $\mu = m$, and the v^2 coefficients c_2 and c_3 can be set to zero. There is no one loop anomalous dimension for the operator $\psi_{\mathbf{p}}\boldsymbol{\sigma}^i \chi_{-\mathbf{p}}^*$, so the LL result is that $c_1 = 1$ at all ν.

At NLL order, we need the one loop matching for c_1 at $\mu = m$, and the two loop running for c_1. The coefficients $c_{2,3}$ first enter at NNLL, at which order one would also need the three-loop anomalous dimension for c_1. At two loops, the anomalous dimension for c_1 was computed at the matching scale $\mu = m$ [20,21]

$$\mu \frac{\partial}{\partial \mu} c_1(\mu) \bigg|_{\mu = m} = -C_F \left(\frac{1}{3} C_F + \frac{1}{2} C_A \right) \alpha_s^2(m), \quad (5)$$

by studying the two loop matching condition for c_1. For $\mu < m$ the anomalous dimension no longer has the simple form Eq. (5), but depends on the running of the quark potential. This anomalous dimension was computed in Ref. [14], and depends on the running values $[\tilde{V}^{(-2,1)}]^2$, $\tilde{V}^{(-2,1)} \times \tilde{V}^{(0,1)}$, and $\tilde{V}^{(-1,2)}$ [see Eq. (42) below]. It is interesting that the structure of this result implies that determining the RHS of Eq. (5) for $\mu < m$ requires the LL values of $\tilde{V}^{(-2,1)}$ and $\tilde{V}^{(0,1)}$, but the NLL value of $\tilde{V}^{(-1,2)}$. The one loop running of

$\tilde{V}^{(-2,1)}$ is well known, and the running of $\tilde{V}^{(-2,2)}$ was computed in Refs. [18,19]. The two loop running of $\tilde{V}^{(-1,2)}$ is computed in this paper. Using the running of these terms in the potential, we arrive at a complete NLL expression for c_1. The running of the nonrelativistic scalar current is also briefly discussed.

In Sec. II the effective theory is reviewed. We explain how reparametrization invariance fixes the value of the lowest order coupling of an ultrasoft gluon to the Coulomb potential. The details of the computation of the two loop anomalous dimension for the $1/|\mathbf{k}|$ potential are given in Sec. III, and in the Appendixes. In Sec. III we give a derivation of the anomalous dimension using on-shell potentials, while in Appendix B we repeat the derivation in the presence of off-shell potentials. Readers not interested in the technical details can skip to Sec. IV, where our results are discussed. In Sec. IV we expand our renormalization group improved results in powers of α_s to compare to finite order calculations in the literature. For the color singlet $1/|\mathbf{k}|$ potential the first $\alpha_s \ln(v)$ term in the series was computed in Ref. [15], and our result for this term agrees with theirs. In Ref. [22], Kniehl and Penin computed the $\alpha_s^3 \ln^2(\alpha_s)$ terms in the wave function at the origin which they refer to as ''nonrenormalization group logarithms,'' since they do not involve factors of the β function for α_s. We show that the second term in the series generated by our NLL production current agrees with the result in Ref. [22]. Thus, the solution of the renormalization group equations in the velocity renormalization group method does include these logarithms. Finally, we discuss our result for the NLL $1/|\mathbf{k}|$ potential and production current.

II. THE vNRQCD LAGRANGIAN

The vNRQCD effective Lagrangian has the form [14]

$$\mathcal{L} = \mathcal{L}_u + \mathcal{L}_p + \mathcal{L}_s. \quad (6)$$

The ultrasoft Lagrangian $\mathcal{L}_u$ involves the fields $\psi_{\mathbf{p}}$ which annihilate a quark, $\chi_{\mathbf{p}}$ which annihilate an antiquark, and A^μ which annihilate and create ultrasoft gluons. The potential Lagrangian $\mathcal{L}_p$ contains operators with four or more quark fields including the quark-antiquark potential. Finally, the soft Lagrangian $\mathcal{L}_s$ contains all terms that involve soft particles which have energy and momenta of order mv. The terms we need in the ultrasoft Lagrangian include

$$\mathcal{L}_u = -\frac{1}{4} F^{\mu\nu} F_{\mu\nu} + \sum_{\mathbf{p}} \psi_{\mathbf{p}}^\dagger \left\{ iD^0 - \frac{(\mathbf{p} - i\mathbf{D})^2}{2m} + \frac{\mathbf{p}^4}{8m^3} \right\} \psi_{\mathbf{p}}$$
$$+ \sum_{\mathbf{p}} \chi_{\mathbf{p}}^\dagger \left\{ iD^0 - \frac{(\mathbf{p} - i\mathbf{D})^2}{2m} + \frac{\mathbf{p}^4}{8m^3} \right\} \chi_{\mathbf{p}}. \quad (7)$$

The covariant derivative is $D^\mu = \partial^\mu + ig\mu_U^\epsilon A^\mu = (D^0, -\mathbf{D})$, so that $D^0 = \partial^0 + ig\mu_U^\epsilon A^0$, $\mathbf{D} = \boldsymbol{\nabla} - ig\mu_U^\epsilon \mathbf{A}$, and involves only the ultrasoft gluon fields. The ultrasoft scale parameter $\mu_U = mv^2$, where $\nu \sim v$ is the subtraction velocity. This v

---
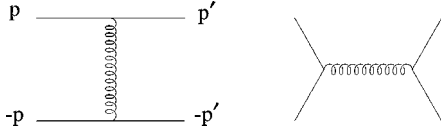
[2] We will ignore effects associated with the top quark width.

FIG. 1. QCD diagrams for tree level matching.

FIG. 2. Matching for the operator attaching an ultrasoft gluon to a potential interaction.

scaling for μ_U is required for a consistent power counting in d dimensions [23]. The covariant derivative on $\psi_{\mathbf{p}}$ and $\chi_{\mathbf{p}}$ contain the color matrices T^A and $\bar{T}^A$ for the **3** and $\bar{\mathbf{3}}$ representations, respectively.

The Lagrangian $\mathcal{L}_p$ includes both the traditional quark potential and ultrasoft corrections to this potential which we will denote by $\mathcal{L}_{pu}$:

$$\mathcal{L}_p = -\sum_{\mathbf{p},\mathbf{p}'} V_{\alpha\beta\lambda\tau}(\mathbf{p},\mathbf{p}')\mu_S^{2\epsilon}\psi_{\mathbf{p}'\,\alpha}^\dagger\psi_{\mathbf{p}\beta}\chi_{-\mathbf{p}'\lambda}^\dagger\chi_{-\mathbf{p}\tau} + \mathcal{L}_{pu}. \tag{8}$$

The terms we need in $\mathcal{L}_{pu}$ are fixed by reparametrization invariance [24] and will be described below. The on-shell potential $V(\mathbf{p},\mathbf{p}')_{\alpha\beta\lambda\tau}$ has an expansion in α_s and v, and α, β, λ, τ denote color and spin indices. We will use the color basis in which the potential V is written as a linear combination of $1\otimes1$ and $T\otimes\bar{T}$. The tree level diagrams in Fig. 1 generate terms of $\mathcal{O}(v^{2k}\alpha_s)$ in the QCD potential. The order v^{-2} Coulomb potential is

$$V^{(-2)} = (T^A\otimes\bar{T}^A)\frac{\mathcal{V}_c^{(T)}}{\mathbf{k}^2} + (1\otimes1)\frac{\mathcal{V}_c^{(1)}}{\mathbf{k}^2}, \tag{9}$$

where the coefficients $\mathcal{V}_c^{(T,1)}$ have an expansion in α_s. The order v^0 potential includes

$$V^{(0)} = (T^A\otimes\bar{T}^A)\left[\frac{\mathcal{V}_2^{(T)}}{m^2} + \frac{\mathcal{V}_r^{(T)}(\mathbf{p}^2+\mathbf{p}'^2)}{2m^2\mathbf{k}^2} + \frac{\mathcal{V}_s^{(T)}}{m^2}\mathbf{S}^2 \right.$$
$$\left. + \frac{\mathcal{V}_\Lambda^{(T)}}{m^2}\Lambda(\mathbf{p}',\mathbf{p}) + \frac{\mathcal{V}_t^{(T)}}{m^2}T(\mathbf{k})\right]$$
$$+ (1\otimes1)\left[\frac{\mathcal{V}_2^{(1)}}{m^2} + \frac{\mathcal{V}_s^{(1)}}{m^2}\mathbf{S}^2\right], \tag{10}$$

where $\mathbf{k}=\mathbf{p}'-\mathbf{p}$ and

$$\mathbf{S} = \frac{\boldsymbol{\sigma}_1+\boldsymbol{\sigma}_2}{2}, \quad \Lambda(\mathbf{p}',\mathbf{p}) = -i\frac{\mathbf{S}\cdot(\mathbf{p}'\times\mathbf{p})}{\mathbf{k}^2},$$

$$T(\mathbf{k}) = \boldsymbol{\sigma}_1\cdot\boldsymbol{\sigma}_2 - \frac{3\mathbf{k}\cdot\boldsymbol{\sigma}_1\mathbf{k}\cdot\boldsymbol{\sigma}_2}{\mathbf{k}^2}. \tag{11}$$

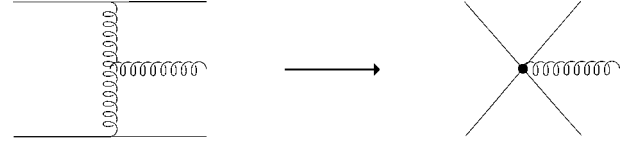Matching the two diagrams in Fig. 1 to the v^{-2} and v^0 potentials at $\mu=m$ gives

$$\mathcal{V}_c^{(T)} = 4\pi\alpha_s(m), \quad \mathcal{V}_r^{(T)} = 4\pi\alpha_s(m),$$

$$\mathcal{V}_s^{(T)} = -\frac{4\pi\alpha_s(m)}{3} + \frac{1}{N_c}\pi\alpha_s(m),$$

$$\mathcal{V}_\Lambda^{(T)} = -6\pi\alpha_s(m), \quad \mathcal{V}_t^{(T)} = -\frac{\pi\alpha_s(m)}{3},$$

$$\mathcal{V}_s^{(1)} = \frac{(N_c^2-1)}{2N_c^2}\pi\alpha_s(m),$$

$$\mathcal{V}_c^{(1)} = 0, \quad \mathcal{V}_2^{(T)} = 0, \quad \mathcal{V}_2^{(1)} = 0. \tag{12}$$

The LL values for the coefficients of the $V^{(-2)}$ and $V^{(0)}$ potentials will be needed below and are summarized in Appendix A. They are obtained by using the tree-level matching values in Eq. (12) and running using the one loop anomalous dimensions computed in Ref. [19].

The order $1/v$ potential includes

$$V^{(-1)} = \frac{\pi^2}{m|\mathbf{k}|}[\mathcal{V}_k^{(T)}(T^A\otimes\bar{T}^A) + \mathcal{V}_k^{(1)}(1\otimes1)]. \tag{13}$$

Tree level matching gives $V^{(-1)}=0$, and $V^{(-1)}$ has zero one loop anomalous dimension [19], so $V^{(-1)}=0$ at LL order as well. At one loop in QCD, order $1/v$ potentials of the form in Eq. (13) are generated. The one loop matching of the on-shell potential at $\mu=m$ gives [23]

$$\mathcal{V}_k^{(T)} = \alpha_s^2(m)\left(\frac{7C_A}{8} - \frac{C_d}{8}\right), \quad \mathcal{V}_k^{(1)} = \alpha_s^2(m)\frac{C_1}{2}. \tag{14}$$

The color group theory factors are $C_F=(N_c^2-1)/(2N_c)$, $C_A=N_c$, $C_1=(N_c^2-1)/(4N_c^2)$, and $C_d=N_c-4/N_c$. For the color singlet channel Eq. (14) agrees with Refs. [25,26]. In the language of the threshold expansion [10] the value of the coefficients in Eqs. (12) and (14) are from integrating out off-shell potential gluons at the hard scale $\mu\sim m$ where $\nu=1$ [23]. In the next section we will compute the two loop anomalous dimension for $V^{(-1)}$, and determine the NLL value of the coefficients in Eq. (13).

In addition we need ultrasoft corrections to the potential which are contained in $\mathcal{L}_{pu}$. Reparametrization invariance

[24] restricts the form of some of these terms by requiring that only the linear combination $\mathbf{p}-i\mathbf{D}$ can appear. Here the covariant derivative acts on a quark or antiquark field with label $\mathbf{p}$. The reparametrization invariant form of the $T\otimes\bar{T}$ Coulomb potential operator is

$$\frac{[\psi_{\mathbf{p}'}^{\dagger}T^{A}\psi_{\mathbf{p}}][\chi_{-\mathbf{p}'}^{\dagger}\bar{T}^{A}\chi_{-\mathbf{p}}]}{(\mathbf{p}'-\mathbf{p})^{2}}\rightarrow\frac{1}{2}\left[\psi_{\mathbf{p}'}^{\dagger}\frac{T^{A}}{(\mathbf{p}'-\mathbf{p}+i\vec{D})^{2}}\psi_{\mathbf{p}}\right][\chi_{-\mathbf{p}'}^{\dagger}\bar{T}^{A}\chi_{-\mathbf{p}}]+\frac{1}{2}[\psi_{\mathbf{p}'}^{\dagger}T^{A}\psi_{\mathbf{p}}]\left[\chi_{-\mathbf{p}'}^{\dagger}\frac{\bar{T}^{A}}{(-\mathbf{p}'+\mathbf{p}+i\vec{D})^{2}}\chi_{-\mathbf{p}}\right],\quad(15)$$

where $\vec{D}=\vec{D}+\bar{D}$. Terms in the v expansion are then generated by expanding Eq. (15) with $\mathbf{D}\ll\mathbf{p}'-\mathbf{p}$. As written the ordering of color generators in Eq. (15) is ambiguous. The correct ordering in the expansion is to write factors of $\vec{D}$ to the right of the T^{A}, and factors of $\bar{D}$ to the left of the T^{A}. Expanding Eq. (15) and keeping only the terms that we will need gives

$$\mathcal{L}_{pu}=\frac{2i\mathcal{V}_{c}^{(T)}f^{ABC}}{\mathbf{k}^{4}}\mu_{S}^{2\epsilon}\mu_{U}^{\epsilon}\mathbf{k}\cdot(g\mathbf{A}^{C})\psi_{\mathbf{p}'}^{\dagger}T^{A}\psi_{\mathbf{p}}\chi_{-\mathbf{p}'}^{\dagger}\bar{T}^{B}\chi_{-\mathbf{p}}+\mathcal{V}_{c}^{(T)}\mu_{S}^{2\epsilon}\psi_{\mathbf{p}'}^{\dagger}\left[\frac{i\mathbf{k}\cdot\vec{\nabla}}{\mathbf{k}^{4}}-\frac{\vec{\nabla}^{2}}{2\mathbf{k}^{4}}+2\frac{(\mathbf{k}\cdot\vec{\nabla})^{2}}{\mathbf{k}^{6}}\right]T^{A}\psi_{\mathbf{p}}\chi_{-\mathbf{p}'}^{\dagger}\bar{T}^{A}\chi_{-\mathbf{p}}$$

$$+\mathcal{V}_{c}^{(T)}\mu_{S}^{2\epsilon}\psi_{\mathbf{p}'}^{\dagger}T^{A}\psi_{\mathbf{p}}\chi_{-\mathbf{p}'}^{\dagger}\left[\frac{-i\mathbf{k}\cdot\vec{\nabla}}{\mathbf{k}^{4}}-\frac{\vec{\nabla}^{2}}{2\mathbf{k}^{4}}+2\frac{(\mathbf{k}\cdot\vec{\nabla})^{2}}{\mathbf{k}^{6}}\right]\bar{T}^{A}\chi_{-\mathbf{p}},\quad(16)$$

where $\vec{\nabla}=\bar{\nabla}+\vec{\nabla}$. The first term couples an ultrasoft gluon to a four quark operator. The terms in the second and third lines in Eq. (16) contain order $1/v$ and v^{0} terms from the multipole expansion of the Coulomb potential. The first term could also have been determined from the on-shell matching calculation shown in Fig. 2. However, by determining the terms in Eq. (16) using reparametrization invariance rather than matching we know that the coefficients remain equal to $\mathcal{V}_{c}$ to all orders in perturbation theory. This saves us from the extra work that would be involved in computing the anomalous dimensions for these terms in $\mathcal{L}_{pu}$.

The terms in the soft Lagrangian include

$$\mathcal{L}_{s}=\sum_{q}\{|q^{\mu}A_{q}^{\nu}-q^{\nu}A_{q}^{\mu}|^{2}+\bar{\varphi}_{q}\slashed{q}\varphi_{q}+\bar{c}_{q}q^{2}c_{q}\}-g^{2}\mu_{S}^{2\epsilon}\sum_{\mathbf{p},\mathbf{p}'q,q'}\left\{\frac{1}{2}\psi_{\mathbf{p}'}^{\dagger}[A_{q'}^{\mu},A_{q}^{\nu}]U_{\mu\nu}^{(\sigma)}\psi_{\mathbf{p}}+\frac{1}{2}\psi_{\mathbf{p}'}^{\dagger}\{A_{q'}^{\mu},A_{q}^{\nu}\}W_{\mu\nu}^{(\sigma)}\psi_{\mathbf{p}}\right.$$

$$\left.+\psi_{\mathbf{p}'}^{\dagger}[\bar{c}_{q'},c_{q}]Y^{(\sigma)}\psi_{\mathbf{p}}+(\psi_{\mathbf{p}'}^{\dagger}T^{B}Z_{\mu}^{(\sigma)}\psi_{\mathbf{p}})(\bar{\varphi}_{q'}\gamma^{\mu}T^{B}\varphi_{q})\right\}+(\psi\rightarrow\chi,T\rightarrow\bar{T}).\quad(17)$$
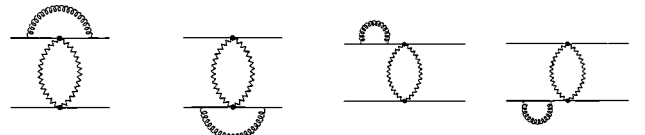
The fields A_{q}^{μ} and c_{q} are the soft gluon and ghost fields, and φ_{q} is a massless soft quark field with n_{f} flavor components. U, W, Y, and Z are functions of $(\mathbf{p},\mathbf{p}',q,q')$ and matrices in spin and the index σ denotes the relative order in the v expansion. For Feynman gauge and the case $\mathbf{p}^{2}=\mathbf{p}'^{2}$ these functions were derived in Refs. [14,19]. Beyond one loop terms proportional to $(\mathbf{p}^{2}-\mathbf{p}'^{2})$ will be needed in $\mathcal{L}_{s}$, since besides its soft energy $q^{0}\sim mv$ the A_{q} gluons can carry away a residual energy of order mv^{2}. The LL values for the functions U, W, Y, and Z can be found in Appendix A of Ref. [23]. In addition, some NLL contributions to $\mathcal{L}_{s}$ will be needed and will be discussed in Sec. III A. These additional contributions are obtained from one loop matching with two-loop renormalization group improvement.

As an aside, note that it is not necessary to consider the ultrasoft renormalization of the vertices given in the soft Lagrangian in Eq. (17). One might think that diagrams such as

 (18)

would affect the running of the coefficients in the soft Lagrangian. Diagrams analogous to the one in Eq. (18), but

with only soft gluons and quarks generate the running of the coefficient functions in the soft Lagrangian[3] in Ref. [19]. However, the graph in Eq. (18) has only one heavy quark, so a distinction between soft and ultrasoft gluons is unnecessary at this point. Noting that the soft vertices will always occur in pairs, it is in fact consistent to only dress pairs of the soft vertices by ultrasoft gluons:

(19)

---

[3]In Ref. [19] the running of $\mathcal{L}_{s}$ was calculated by examining loops with soft gluons that contribute to the Compton scattering process prior to integrating out the soft quarks. There it was noted that all ultraviolet divergent diagrams are in one-to-one correspondence with graphs in heavy quark effective theory (HQET), so that the running of this Lagrangian could be obtained from the known running in HQET [27].
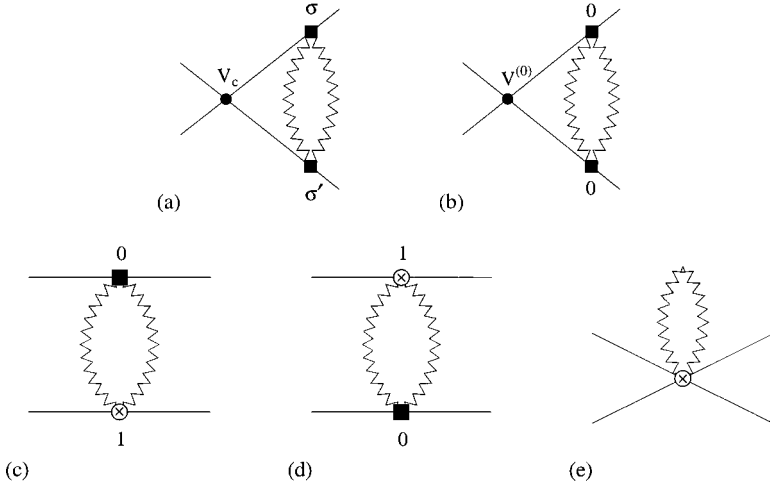
FIG. 3. Order α_s^3/v graphs containing soft gluons, ghosts, or massless quarks which are all denoted by a zigzag line. In (a) the dot denotes the Coulomb potential, while in (b) the dot denotes the order v^0 potential. The boxes denote soft vertices with insertions of the functions $U^{(\sigma)}$, $W^{(\sigma)}$, $Y^{(\sigma)}$, or $Z^{(\sigma)}$. In (a) the indices $\sigma+\sigma' = 2$. In (c), (d), and (e) the $\otimes$ vertex is obtained from the one loop matching in Fig. 4.

Since these diagrams involve two heavy quarks, both types of gluons can occur. Since in the end it is only graphs such as Eq. (19) with two soft vertices that are relevant for constructing the theory, it is consistent to include the ultrasoft renormalization of soft vertices as a contribution to the four-quark operator in Eq. (19), rather than treating the subgraph as a contribution to the soft vertex, as in Eq. (18). Along with the diagrams in Eq. (19) there are graphs in which the ultrasoft gluon is exchanged between the two heavy quarks.

III. TWO LOOP ANOMALOUS DIMENSION FOR $V^{(-1)}$

To calculate the NLL anomalous dimension for the $1/|\mathbf{k}|$ potentials we need to consider graphs in the effective theory of order[4] α_s^3/v. These diagrams come in two classes, those with soft gluons, and those with a single ultrasoft gluon. The total anomalous dimension for the $1/|\mathbf{k}|$ potential is $\gamma^{(1,T)} = \nu d/d\nu \mathcal{V}_k^{(1,T)}$. Since $\mu_S = m\nu$ and $\mu_U = m\nu^2$, $\gamma^{(1,T)}$ can be written as the sum of a soft and ultrasoft anomalous dimension

$$\gamma^{(1,T)} = \gamma_S^{(1,T)} + 2\gamma_U^{(1,T)}, \qquad (20)$$

where $\gamma_S^{(1,T)} = \mu_S \partial/\partial\mu_S \mathcal{V}_k^{(1,T)}$ and $\gamma_U^{(1,T)} = \mu_U \partial/\partial\mu_U \mathcal{V}_k^{(1,T)}$. In the remainder of this section we discuss the computation of these two loop anomalous dimensions in detail. The calculation is split into two parts, graphs with soft vertices and graphs with ultrasoft vertices. Graphs with soft gluons only contribute to γ_S, while those with an ultrasoft gluon contribute to both γ_S and γ_U.

A. Soft contributions

The order α_s^3/v diagrams containing soft gluons that contribute to the anomalous dimension are shown in Fig. 3. The sum of diagrams forms a gauge invariant set.

———————

[4]This is the size (in v) of the amputated diagrams, so in contrast to the general power counting formula in Ref. [14] we are not including the powers of v generated by external lines.

The two loop graphs in Figs. 3(a) and 3(b) involve an iteration of a potential and a soft loop. The vertices in these graphs are of LL order (tree level matching with one loop running) and are given in Ref. [23]. In Figs. 3(a) and 3(b) counting powers of v from the propagators and from the loop measures gives a v^1, so the sum of powers of v for the three (amputated) vertices must give an overall $1/v^2$. The v scaling for the two soft vertices is $\sigma+\sigma'-2$. In Fig. 3 we show two possibilities: (a) has one $V^{(-2)}$ insertion and two soft vertices from Eq. (17) such that $\sigma'+\sigma=2$, and (b) has one insertion of a $V^{(0)}$ potential from Eq. (10) and two soft vertices such that $\sigma'=\sigma=0$. We could also have a $V^{(-1)}$ potential plus two soft vertices where $\sigma+\sigma'=1$; however this diagram is identically zero. The graphs where the potential and soft loop are exchanged simply give a factor of 2.

The one loop graphs in Figs. 3(c), 3(d), and 3(e) involve additional vertices in $\mathcal{L}_s$, denoted $\otimes$, which are of NLL order (from one loop matching with two loop running). The one loop matching calculation for these vertices is sketched in Fig. 4. There are a large number of diagrams in the full theory (graphs on the left-hand side), so only a few representative examples have been shown. To obtain the values for the operators on the right hand side we subtract purely soft effective theory diagrams from those in the full theory. To see how these operators arise, it is useful to recall that in the threshold expansion [7,11] soft heavy quarks have a propagator

$$\frac{1}{q_0+i\epsilon} = P\frac{1}{q_0} - i\pi\delta(q_0), \qquad (21)$$

where P stands for the principal value. In our approach, off-shell potential gluons and soft quarks are integrated out at the scale m when constructing the effective theory. When integrating out the soft heavy quarks the principal value term in Eq. (21) goes directly into a coefficient in the soft Lagrangian since this term is consistent with the scaling in the soft regime, $q_0\sim m v$. For instance, in Eq. (17), $U_{00}^{(0)} = 1/q_0$. The delta function contribution in Eq. (21) is asso-
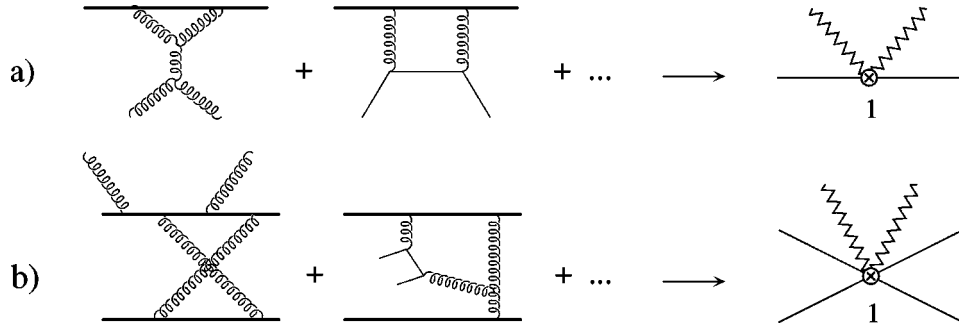
FIG. 4. Contributions to the soft Lagrangian from one loop matching. In the full theory diagrams on the left the thick lines are massive quarks, while the thin lines are massless quarks. The matching in (a) gives α_s corrections to the functions $U^{(1)}$, $W^{(1)}$, $Y^{(1)}$, and $Z^{(1)}$ in Eq. (17). The matching in (b) induces new operators that involve the scattering of soft gluons, ghosts, or light quarks off of a four fermion potential.

ciated with the potential regime since $q_0 \sim 0$. When the delta function appears in a loop in the full theory (or threshold expansion) it forces gluons in the loop to have zero energy, or in other words to become potential gluons. It is these contributions which do not appear in the soft effective theory diagrams and must be made up by the operators shown on the right-hand side of Fig. 4.

The total contribution to the anomalous dimensions from the soft diagrams in Fig. 3 is

$$\gamma_S^{(T)} = -\frac{\beta_0(7C_A - C_d)}{8\pi}\alpha_s^3(m\upsilon) - \frac{8C_A(C_A + C_d)}{3\pi}\alpha_s^3(m\upsilon),$$

$$\gamma_S^{(1)} = -\frac{\beta_0 C_1}{2\pi}\alpha_s^3(m\upsilon) + \frac{16C_A C_1}{\pi}\alpha_s^3(m\upsilon), \quad (22)$$

where $\beta_0 = 11C_A/3 - 4T_F n_f/3$, n_f is the number of massless soft quarks, and $\mathcal{V}_c(\upsilon) = 4\pi\alpha_s(m\upsilon)$ was used. In Eq. (22) the terms proportional to β_0 can be inferred from Eq. (14). They simply turn the $\alpha_s(m)$'s in the matching result into running α_s's. At one and two loops terms proportional to the β-function for α_s completely determine the soft anomalous dimension for the Coulomb potential. However, the $1/|\mathbf{k}|$ potentials have additional contributions because the soft diagrams in Figs. 3(c), 3(d), and 3(e) have infrared divergences. The IR divergences from purely soft diagrams are not true IR divergences in the effective theory. For instance, in general they do not match up with IR divergences in QCD. The true IR divergences are from momenta $< m\upsilon^2$, and the desired ultraviolet divergences are from momenta $\geq m$. Instead, the soft IR divergences are from momenta $< m\upsilon$, and match up with ultrasoft UV divergences that are from momenta $\geq m\upsilon$ to carry these UV divergences up to the hard scale. Writing the soft IR divergence

$$\frac{1}{\epsilon_{IR}} = \frac{1}{\epsilon_{UV}} - \left(\frac{1}{\epsilon_{UV}} - \frac{1}{\epsilon_{IR}}\right), \quad (23)$$

the first term contributes to the anomalous dimension in Eq. (22). The $1/\epsilon_{UV} - 1/\epsilon_{IR}$ term can be ignored since it simply takes the corresponding ultrasoft UV divergence up to the hard scale m.[5] Thus, to compute γ_S, all divergences from soft loops should be treated as UV divergences. The terms not proportional to β_0 in Eq. (22) can be inferred from the result of the ultrasoft calculation in Eq. (30) of the next section.

Despite the fact that Eq. (22) can be inferred without a direct calculation it is worthwhile to examine the diagrams in Fig. 3. Consider the graphs in Figs. 3(a) and 3(b) in Feynman gauge. The subloop with soft gluons is divergent, while the remaining potential loop is convergent. There is also a set of one loop diagrams (not shown) where the soft subloop is replaced by the one loop counterterms for V derived in Ref. [19]. We find that these counterterm graphs exactly cancel against a set of divergences in Figs. 3(a) and 3(b). For Fig. 3(b) there is an exact cancellation, and so there is no operator mixing between $V^{(0)}$ and $V^{(-1)}$. However, there are divergences that appear in Fig. 3(a) that have no corresponding counterterm graphs. Consider the soft gluon case (the ghost and soft quark cases are similar). After performing the k^0 integration the loop integral for Fig. 3(a) is

$$\int d^{d-1}\mathbf{q} \frac{1}{(E - \mathbf{q}^2/m)(\mathbf{p} - \mathbf{q})^2}$$

$$\times \left[\int d^d t \frac{U_{\mu\nu}^{(\sigma)} U^{\mu\nu(\sigma')}}{t^2[(t^0)^2 - (\mathbf{t} + \mathbf{q} - \mathbf{p}')^2]}\right], \quad (24)$$

where $\mathbf{p}$ and $\mathbf{p}'$ are the momenta of the incoming and outgoing quarks, $E = \mathbf{p}^2/m$ and in Eq. (24) the U's depend on $\mathbf{q}$,

---

[5]This result, that there are no true IR divergences in the soft regime has not been proven to all orders in perturbation theory. However, its is likely that all IR divergences can be attributed to ultrasoft and collinear gluons in the spirit of the Coleman-Norton theorem [28], plus IR divergences associated with the Coulomb regime that are reproduced by iterations of the potential.

t, **p**′, and t^0. For the divergences of interest performing the t integral (the soft loop) in $d = 4 - 2\epsilon$ dimensions gives a factor of

$$\frac{(\mathbf{p}'^2 - \mathbf{q}^2)^2}{m^2 (\mathbf{p}' - \mathbf{q})^{4+2\epsilon} \epsilon} + \cdots, \tag{25}$$

where the ellipsis denotes order ϵ^0 terms. The remaining loop integration is finite. For the one loop graph that corresponds to the soft sub-loop, the loop momenta **q** in Eq. (25) is replaced by **p**′, and this diagram vanishes on-shell by energy conservation so no counterterm is generated. Performing the final integration and including the factor of 2 from the left-right symmetric graph gives

$$\text{Fig. } 3(a) = i\mathcal{V}_c^{(T)}(\mu_S) \alpha_s^2(\mu_S) \frac{\beta_0 \mu_S^{2\epsilon}}{32m|\mathbf{k}|} (T^A T^B \otimes \bar{T}^A \bar{T}^B)$$

$$\times \left[\frac{1}{\epsilon} + 2 \ln\left(\frac{\mu_S^2}{|\mathbf{k}|^2} \right) + \cdots \right]. \tag{26}$$

The divergence in Eq. (26) contributes to the anomalous dimension for $\mathcal{V}_k$. This seems slightly unusual because it was generated by a subdivergence, whereas usually only the overall divergence in a diagram is relevant. In this diagram the loop integral with soft gluons generates a $1/\epsilon$ pole, and the remaining potential loop integral generates the $1/|\mathbf{k}|$ factor. The corresponding diagrams in QCD include graphs such as the vacuum polarization of one of the gluons in the box diagram. In this full theory graph the subdivergence due to the vacuum polarization insertion would be canceled by a counterterm. However, in the effective theory this divergence is instead absorbed into the coefficients of terms in the quark potential because the potential gluon components have been integrated out. Since matching the full theory box diagram gives a contribution to the $1/|\mathbf{k}|$ potential, it is not surprising that gluon vacuum polarization in the box graph contributes to the anomalous dimension of this potential. An alternative to the approach used to derive Eq. (26) is to use off-shell matching and running. In this case the soft anomalous dimension analysis will be different (since, for instance, the off-shell potential is gauge dependent). This approach is discussed in Appendix B, where it is shown that the final answer for physical observables is unchanged.

The diagrams in Figs. 3(c), 3(d), and 3(e) are tedious to evaluate due to the large number of diagrams necessary for the matching calculation in Fig. 4.[6] Since the graphs in Figs. 3(c), 3(d), and 3(e) are one-loop diagrams there is no cancellation from counterterms. In Feynman gauge

---

[6]In fact once a contribution to $\otimes$ has been identified it is simpler to directly evaluate the two-loop diagram obtained by combining the steps in Fig. 4 and Fig. 3.

$$\text{Figs. } 3c, d, e = i \frac{\pi^2 \mu_S^{2\epsilon}}{m|\mathbf{k}|} \frac{\alpha_s^2(\mu_S)}{4\pi\epsilon} \left\{ \frac{4}{3} C_1 T_F n_f (1 \otimes 1) \right.$$

$$+ \left(C_A T_F n_f - \frac{1}{3} C_d T_F n_f \right) (T^A \otimes \bar{T}^A)$$

$$+ \frac{37}{3} C_A C_1 (1 \otimes 1) - \left(\frac{7}{4} C_A C_d + \frac{65}{12} C_A^2 \right)$$

$$\left. \times (T^A \otimes \bar{T}^A) \right\}. \tag{27}$$

Only the terms proportional to n_f in Eq. (27) have been checked by direct calculation. Also, in Eq. (27) we have assumed that the $\otimes$ operators simply run with the strong coupling constant, $\alpha_s(m\nu)$. To motivate this, recall that a theory of propagating soft quarks and gluons has the same singularity structure as heavy quark effective theory (HQET). The operators that are generated in Fig. 4 correspond to diagrams in HQET with insertions of $\nabla^2/(m)$ or a $\mathbf{p} \cdot \mathbf{A}/m$ vertex. Since these operators do not run in HQET the operators that are constructed in Fig. 4 should also simply run with the strong coupling constant.

B. Ultrasoft contributions

Next consider the order α_s^3/v diagrams with ultrasoft gluons. At one loop we have a single insertion of the $V^{(-1)}$ potential dressed by an ultrasoft gluon with gA^0 couplings. These diagrams are obviously zero in Coulomb gauge and in Feynman gauge it was shown in Ref. [14] that, with any potential, the sum of this set of one loop diagrams is also identically zero. At two loops in an arbitrary gauge there are many possible contributions. There are diagrams with two $V^{(-2)}$ vertices, and an ultrasoft tadpole generated by the seagull $\mathbf{A}^2$ operator attached to one of the quark lines. These graphs do not have logarithmic divergences and therefore do not contribute to the anomalous dimension. There are also diagrams that are zero because they are odd in an ultrasoft momenta which we can omit. Next consider the topologies shown in Fig. 5. Several classes of diagrams are generated depending on the vertices used: (1) vertex 1 and 2 are $V^{(-2)}$, and the ultrasoft gluon couples with $\mathbf{p} \cdot \mathbf{A}/m$; (2) vertex 1 and 2 are $V^{(-2)}$, the ultrasoft gluon couples with gA^0, and there are two insertions of $\mathbf{p} \cdot \nabla/m$ on quark lines; (3) vertex 1 and 2 are $V^{(-2)}$, the ultrasoft gluon couples with gA^0, and there is one insertion of ∇^2/m on a quark line; (4) vertex 1 and 2 are $V^{(-2)}$, the ultrasoft gluon couples with gA^0, and there is one insertion of $\mathbf{p}^4/m^3$ on a quark line (together with the expansion of factors of the energy that appear in lower order diagrams which should be viewed as corrections to the effective theory states, see Refs. [7,23]); (5) vertex 1 is $V^{(-2)}$, vertex 2 is $V^{(0)}$ and the ultrasoft gluon couples with gA^0; (6) vertex 1 is the order $1/v$ potential from the multipole expansion of the Coulomb potential given in Eq. (16), vertex 2 is $V^{(-2)}$, and the ultrasoft gluon couples with gA^0 vertices; (7) vertex 1 is the order v^0 potential in Eq. (16), vertex 2 is $V^{(-2)}$, there is one insertion of $\mathbf{p} \cdot \nabla/m$ on a quark line, and the ultrasoft gluon couples with gA^0 vertices; (8) vertex 1 and 2 are v^0 potentials from Eq. (16), and the ultrasoft gluon
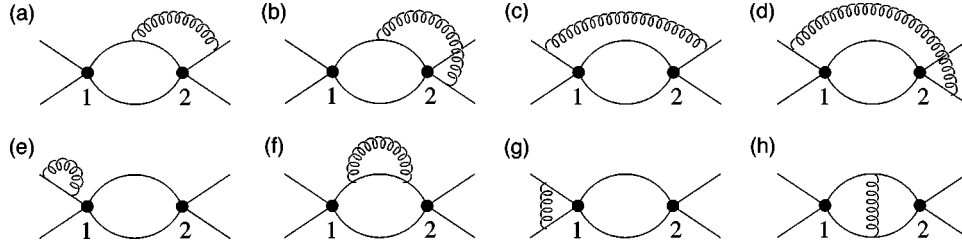
FIG. 5. Order α_s^3/v two loop graphs with an ultrasoft gluon and two potential insertions. The topologies shown give several different classes of diagrams depending on the vertices used as explained in the text. The diagrams obtained by flipping the graphs left-to-right and up-to-down are to be understood.

couples with gA^0 vertices. Insertions of operators with $\boldsymbol{\nabla}$'s only need to be considered on quark propagators where the multipole expansion was used; together with the graphs in cases (6), (7), and (8) they build up the subleading terms in the multipole expansion.

The graphs in cases (1), (2), and (5) do not give any contribution to the two loop anomalous dimension. The reason is that all ultraviolet divergences are exactly canceled by one loop counterterm graphs (these counterterms are generated by one loop graphs having one potential insertion dressed by an ultrasoft gluon, and in Feynman gauge were calculated in Refs. [14,19]). The graphs with the topology in Figs. 5(c) and 5(d) are ultraviolet finite. For the remaining diagrams we can identify the corresponding counterterm graph by simply shrinking the smallest loop containing the ultrasoft gluon to a point. The only subtlety occurs in Fig. 5(h) which has overlapping potential and ultrasoft loop integrals. For heavy scalars this graph was analyzed in Ref. [10] with the threshold expansion, while in an effective theory for heavy fermions this diagram was analyzed in Ref. [29] for the case where the ultrasoft gluon is massive and couples with derivatives at the vertices. Since the nature of the overlapping integrals does not depend on the structure of the numerator or on having a massive gluon, this analysis will not be repeated here. In the effective theory this diagram comes with the appropriate factor of 2, so that it is canceled

by the two one loop counterterm graphs that correspond to either making the loop integral on the right large or making the loop integral on the left large. Note that for a ϕ^3 relativistic theory in $d=6$ [30], the subdivergences for this diagram are also canceled in this way, but leave an overall divergence. For the nonrelativistic effective theory diagram this overall divergence is not present.

For the graphs in case (4), the sum of insertions on quark lines inside the loop shared by the ultrasoft gluon are finite. The graphs with insertions on quark lines outside this loop are ultraviolet divergent, but are exactly canceled by the counterterm diagrams that correspond to shrinking the ultrasoft loop to a point. Therefore, the graphs in case (4) also do not contribute to the anomalous dimension.

In a general gauge the graphs in cases (3), (6), (7), and (8) will contribute to the anomalous dimension. There are also additional graphs with the vertex in Eq. (15) which involves the coupling of an ultrasoft $\mathbf{A}^i$ gluon to a potential vertex. Together this set of graphs gives a gauge invariant contribution to the anomalous dimension, so we can simplify their computation by choosing the most convenient gauge. We will choose Coulomb gauge since the graphs in cases (3), (6), (7), and (8) involve ultrasoft A^0 gluons and vanish in this gauge. The result for the infinite part of the the remaining diagrams in Coulomb gauge is

$$
\text{(graph)} = 0,
\tag{28a}
$$

$$
\text{(graph)} = \frac{-i\,\alpha_s(\mu_U)\mu_S^{2\epsilon}\,[\mathcal{V}_c^{(T)}]^2}{8\pi\,m\,|\mathbf{k}|\,\epsilon}\left[C_A C_1\,1\otimes 1 - \frac{1}{4}C_A(C_A+C_d)T^A\otimes\bar{T}^A\right],
\tag{28b}
$$

$$
\text{(graph)} = \frac{-i\,\alpha_s(\mu_U)\mu_S^{2\epsilon}\,[\mathcal{V}_c^{(T)}]^2}{8\pi\,m\,|\mathbf{k}|\,\epsilon}\,\frac{C_A C_1}{3}\,1\otimes 1,
\tag{28c}
$$

$$
\text{(graph)} = \frac{-i\,\alpha_s(\mu_U)\mu_S^{2\epsilon}\,[\mathcal{V}_c^{(T)}]^2}{8\pi\,m\,|\mathbf{k}|\,\epsilon}\left[\frac{2}{3}C_A C_1\,1\otimes 1 - \frac{1}{12}C_A(C_A+C_d)T^A\otimes\bar{T}^A\right].
\tag{28d}
$$

Equations (28b) and (28c) include the factor of four from their left-right and up-down mirror graphs. In the graphs in Eqs. (28a)–(28d) the factor

$$\frac{\mu_U^{2\epsilon}\mu_S^{4\epsilon}}{\epsilon|\mathbf{k}|^{1+2\epsilon}E^{2\epsilon}} = \frac{\mu_S^{2\epsilon}}{|\mathbf{k}|}\left[\frac{1}{\epsilon} + \ln\left(\frac{\mu_S^2}{|\mathbf{k}|^2}\right) + \ln\left(\frac{\mu_U^2}{E^2}\right)\right] \quad (29)$$

occurs, where $E = \mathbf{p}^2/m$. The first term is included in the result displayed in Eqs. (28a)–(28d), and the remaining terms are not shown. For $\nu \sim v$, we have $\mu_S \sim |k| \sim mv$, $\mu_U \sim E \sim mv^2$, so the soft and ultrasoft scale factors correctly minimize possible large logarithms in the effective theory.

From the sum of diagrams in Eqs. (28a)–(28d) we have the following result for the soft and ultrasoft anomalous dimensions of the order $1/|\mathbf{k}|$ potentials:

$$\gamma_S^{(T)} = \gamma_U^{(T)} = C_A(C_A + C_d)\frac{\alpha_s(m\nu^2)[\mathcal{V}_c^{(T)}(\nu)]^2}{12\pi^3},$$

$$\gamma_S^{(1)} = \gamma_U^{(1)} = -C_A C_1\frac{\alpha_s(m\nu^2)[\mathcal{V}_c^{(T)}(\nu)]^2}{2\pi^3}. \quad (30)$$

Recall that the soft and ultrasoft anomalous dimensions are given by differentiating with respect to $\ln\mu_S$ and $\ln\mu_U$ respectively.

It is interesting to ask how the result in Eq. (30) would be reproduced if terms that vanish by the equations of motion were included in our effective Lagrangian. It is possible to include a term in our effective Lagrangian which makes the graph in Eq. (28b) give no contribution to the anomalous dimension, but the final result for observables remains invariant. This example is discussed in Appendix B.

IV. RESULTS

In this section the NLL heavy quark $1/|\mathbf{k}|$ potential and production current are discussed. After presenting the renormalization group improved results, we reexpand to compare to the finite order results in Refs. [15] and [22]. We also discuss the behavior of the NLL $1/|\mathbf{k}|$ potential and the NLL production current as we run down from $\nu = 1$ to $\nu = v$, where v is the Coulombic velocity.

A. The NLL $1/|\mathbf{k}|$ potentials

The total soft and ultrasoft anomalous dimensions for the on-shell $1/|\mathbf{k}|$ potentials are obtained by adding Eqs. (22) and (30). Using the LL coefficient for the Coulomb potential, $\mathcal{V}_c(\nu) = 4\pi\alpha_s(m\nu)$, we find

$$\gamma_S^{(T)} = -\frac{1}{8\pi}\beta_0(7C_A - C_d)[\alpha_s(m\nu)]^3$$

$$-\frac{8}{3\pi}C_A(C_A + C_d)[\alpha_s(m\nu)]^3$$

$$+\frac{4}{3\pi}C_A(C_A + C_d)\alpha_s(m\nu^2)[\alpha(m\nu)]^2, \quad (31)$$

$$\gamma_S^{(1)} = -\frac{1}{2\pi}\beta_0 C_1[\alpha_s(m\nu)]^3 + \frac{16}{\pi}C_A C_1[\alpha_s(m\nu)]^3$$

$$-\frac{8}{\pi}C_A C_1\alpha_s(m\nu^2)[\alpha_s(m\nu)]^2,$$

$$\gamma_U^{(T)} = \frac{4}{3\pi}C_A(C_A + C_d)\alpha_s(m\nu^2)[\alpha_s(m\nu)]^2,$$

$$\gamma_U^{(1)} = -\frac{8}{\pi}C_A C_1\alpha_s(m\nu^2)[\alpha_s(m\nu)]^2.$$

In full QCD (taking the QCD scale parameter $\mu = m$), the first logarithm generated by the ultrasoft anomalous dimension corresponds to a $\ln(E/m)$, while the first logarithm generated by the soft anomalous dimension corresponds to a $\ln(|\mathbf{k}|/m)$. For the velocity renormalization group, the total anomalous dimension is simply $\gamma_S + 2\gamma_U$:

$$\nu\frac{\partial}{\partial\nu}\mathcal{V}_k^{(T)}(\nu) = -\frac{1}{8\pi}\beta_0(7C_A - C_d)[\alpha_s(m\nu)]^3$$

$$-\frac{8}{3\pi}C_A(C_A + C_d)[\alpha_s(m\nu)]^3$$

$$+\frac{4}{\pi}C_A(C_A + C_d)\alpha_s(m\nu^2)[\alpha(m\nu)]^2,$$

$$\nu\frac{\partial}{\partial\nu}\mathcal{V}_k^{(1)}(\nu) = -\frac{1}{2\pi}\beta_0 C_1[\alpha_s(m\nu)]^3$$ (32)

$$+\frac{16}{\pi}C_A C_1[\alpha_s(m\nu)]^3$$

$$-\frac{24}{\pi}C_A C_1\alpha_s(m\nu^2)[\alpha_s(m\nu)]^2.$$

Note that no other $1/v$ potentials are generated for $\nu < 1$ by operator mixing. Integrating Eq. (32) using the one loop β-function for α_s and the one loop boundary condition in Eq. (14) gives

$$\mathcal{V}_k^{(T)}(\nu) = \frac{(7C_A - C_d)}{8}\alpha_s^2(m)$$

$$+\left[\frac{(7C_A - C_d)}{8} + \frac{8C_A(C_A + C_d)}{3\beta_0}\right](z^2 - 1)\alpha_s^2(m)$$

$$+\frac{8C_A(C_A + C_d)}{\beta_0}[z - 1 - 2\ln(w)]\alpha_s^2(m),$$

$$\mathcal{V}_k^{(1)}(\nu) = \frac{C_1}{2}\alpha_s^2(m) + \left[\frac{C_1}{2} - \frac{16C_A C_1}{\beta_0}\right](z^2 - 1)\alpha_s^2(m)$$ (33)

$$-\frac{48C_A C_1}{\beta_0}\alpha_s^2(m)[z - 1 - 2\ln(w)],$$

where

$$z = \frac{\alpha_s(m\nu)}{\alpha_s(m)}, \quad w = \frac{\alpha_s(m\nu^2)}{\alpha_s(m\nu)} = \frac{1}{2-z}. \quad (34)$$

Projecting onto the color singlet channel, $\mathcal{V}^{(s)} = \mathcal{V}^{(1)} - C_F \mathcal{V}^{(T)}$, and setting $C_d = 8C_F - 3C_A$ and $C_1 = C_A C_F/2 - C_F^2$ gives

$$\mathcal{V}_k^{(s)}(\nu) = \left(\frac{C_F^2}{2} - C_F C_A\right)\alpha_s^2(m)$$
$$+ \left[\frac{C_F^2}{2} - C_F C_A - \frac{8C_A C_F(C_A + 2C_F)}{3\beta_0}\right]$$
$$\times (z^2 - 1)\alpha_s^2(m) - \frac{8C_A C_F(C_A + 2C_F)}{\beta_0}$$
$$\times [z - 1 - 2\ln(w)]\alpha_s^2(m). \quad (35)$$

The projection onto the color octet channel is $\mathcal{V}_k^{(0)} = \mathcal{V}_k^{(1)} + (C_A/2 - C_F)\mathcal{V}_k^{(T)}$.

Logarithmic corrections to the color singlet $V^{(-1)}$ potential were also considered by Brambilla *et al.* [15] using pNRQCD, but were not resummed. Brambilla *et al.* have

$$\mathcal{V}_k^{(s)}(\nu) = -C_F C_A \alpha_s^2(r)$$
$$- \frac{4C_A C_F(C_A + 2C_F)}{3\pi}\alpha_s(\mu)\alpha_s(r)^2 \ln(\mu r). \quad (36)$$

To compare this expression to ours: $\alpha(r) \to \alpha(m\nu)$, $r \to 1/(m\nu)$ and $\mu = \mu_U = m\nu^2$ since r corresponds to the soft scale and μ corresponds to the ultrasoft scale. Expanding Eq. (36) in $\alpha_s(m)$ gives

$$\mathcal{V}_k^{(s)}(\nu) = -C_F C_A \alpha_s^2(m) + \frac{\beta_0 C_F C_A}{\pi}\alpha_s^3(m)\ln[1/(mr)]$$
$$- \frac{4C_A C_F(C_A + 2C_F)}{3\pi}\alpha_s^3(m)\ln(\mu r) + \cdots. \quad (37)$$

To compare this to our result we expand the resummed logarithms in Eq. (35):

$$\mathcal{V}_k^{(s)}(\nu) = \left(\frac{C_F^2}{2} - C_F C_A\right)\alpha_s^2(m) + \frac{\beta_0 C_F C_A}{\pi}\alpha_s^3(m)\ln(\nu)$$
$$- \frac{\beta_0 C_F^2}{2\pi}\alpha_s^2(m)\ln(\nu)$$
$$- \frac{4C_A C_F(C_A + 2C_F)}{3\pi}\alpha_s(m)^3 \ln(\nu) + \cdots. \quad (38)$$

In Eq. (38), the first and second $\ln(\nu)$ terms are entirely from the soft anomalous dimension in Eq. (31), while the third $\ln(\nu)$ term is from a combination of the ultrasoft and soft anomalous dimensions. The first $\ln(\nu)$ term in Eq. (38)
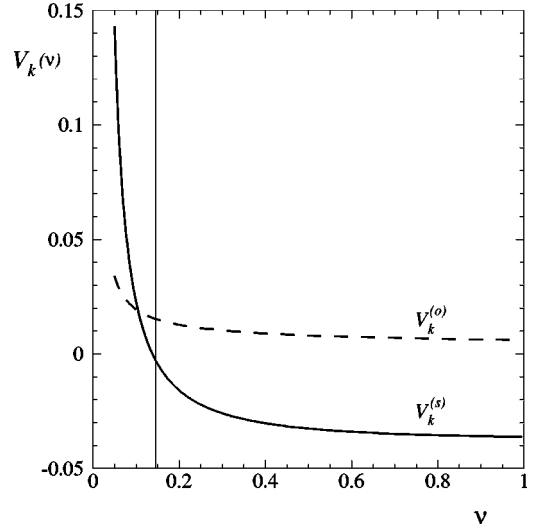

FIG. 6. Values for the NLL running $V^{(-1)}$ potential for top quarks and $n_f = 5$ massless flavors. The solid and dashed lines are the color singlet and octet coefficients for the $\pi^2/(m|\mathbf{k}|)$ potential. The solid vertical line marks the Coulombic regime where $\alpha_s(m\nu) = \nu$.

agrees with the $\ln[1/(mr)] = \ln(\nu)$ term in Eq. (37), and the third $\ln(\nu)$ term in Eq. (38) agrees with the $\ln(\mu r) = \ln(\nu)$ term in Eq. (37).

The second term in Eq. (38) does not appear in Brambilla *et al.*'s expression in Eq. (37). This is because it depends on whether an on-shell or off-shell potential is used for the matching and running.[7] We have used an on-shell potential, while Ref. [15] uses off-shell Coulomb gauge which includes a $\mathcal{V}_{\Delta 2}^{(T)} = -4\pi\alpha_s(r)$ potential as defined in Eq. (B1) of Appendix B. The second logarithm in Eq. (38) should appear from the coefficient of this potential. Transforming Brambilla *et al.*'s $\mathcal{V}_{\Delta 2}^{(T)}$ potential to a $\mathcal{V}_k^{(s)}$ potential using Eq. (B4) gives

$$\mathcal{V}_k^{(s)}(\nu) = \frac{C_F^2}{2}\alpha_s(r)^2$$
$$= \frac{C_F^2}{2}\alpha_s^2(m) - \frac{\beta_0 C_F^2}{2\pi}\alpha_s^3(m)\ln[1/(mr)] + \cdots. \quad (39)$$

The term with a $\ln[1/(mr)] = \ln(\nu)$ agrees with the second $\ln(\nu)$ term in Eq. (38). The sum of terms without logarithms in Eqs. (37) and (39) also agrees with Eq. (38). Note that the next term in the series in Eq. (38) does not give agreement with Eqs. (37) and (39) since Brambilla *et al.* did not attempt to systematically sum all the logarithms.

---

[7] The issue of on-shell versus off-shell potential was discussed in Ref. [23], and in the context of the leading log summation is discussed further in Appendix B.

To see the effect of the running on the value of the $V^{(-1)}$ potential, consider the case of top quark production near threshold. Using $\alpha_s(m_t) = 0.108$ and Eq. (35), the one loop matching value is

$$\mathcal{V}_k^{(s)}(1) = -0.0362. \tag{40}$$

For a Coulombic system we determine the velocity v by solving $\alpha_s(mv) = v$. Using $m_t = 175$ GeV and the one loop running of $\alpha_s(\mu)$ with $n_f = 5$ gives $v = 0.145$. The NLL color singlet and octet coefficients for the $1/|\mathbf{k}|$ potential are plotted in Fig. 6. At $\nu = v$ the running coupling is

$$\mathcal{V}_k^{(s)}(v) = -0.0027, \tag{41}$$

which is a substantial change from Eq. (40). In comparison, the terms shown in Eq. (38) where the combination $\alpha_s \ln(v)$ is treated perturbatively give $\mathcal{V}_k^{(s)}(v) = -0.0313$. Thus, the summation of logarithms for the $1/|\mathbf{k}|$ potential is quite important; it decreases the coefficient by an order of magnitude. Using the unexpanded results in Eqs. (36) and (39) gives $\mathcal{V}_k^{(s)}(v) = 0.0201$, so our resummed result is also quite different from the fixed order result in Ref. [15].

B. The NLL $t\bar{t}$ production current

In terms of the running color singlet potentials the anomalous dimension for the production current in Eq. (4) is [14]

$$\gamma_{c1}(\nu) = \nu \frac{\partial}{\partial \nu} \ln[c_1(\nu)]$$

$$= -\frac{\mathcal{V}_c^{(s)}(\nu)}{16\pi^2} \left(\frac{\mathcal{V}_c^{(s)}(\nu)}{4} + \mathcal{V}_2^{(s)}(\nu) \right.$$

$$\left. + \mathcal{V}_r^{(s)}(\nu) + \mathbf{S}^2 \mathcal{V}_s^{(s)}(\nu) \right) + \frac{\mathcal{V}_k^{(s)}(\nu)}{2}. \tag{42}$$

For the vector production current in Eq. (4) only spin-1 states are produced, and we can set $\mathbf{S}^2 = S(S+1) = 2$. However, our analysis also applies to the scalar production current

$$c(\nu) \sum_{\mathbf{p}} \psi_{\mathbf{p}}^\dagger \chi_{-\mathbf{p}}^*, \tag{43}$$

which, for example, contributes to the process $\gamma\gamma \to t\bar{t}$ [31]. Therefore, we will keep the factors of $\mathbf{S}^2$ explicit in our results. The boundary condition is given by the matching condition at $\nu = 1$ ($\mu = m$) which is known to two loops [21]. For the NLL approximation only the one loop matching condition should be used. For the vector current

$$c_1(1) = 1 - \frac{2 C_F \alpha_s(m)}{\pi}. \tag{44}$$

Integrating Eq. (42) with the running potentials in Appendix A, Eq. (A1) and in Eq. (33) we find

$$\ln\left[\frac{c_1(\nu)}{c_1(1)} \right] = a_1 \pi \alpha_s(m) \left(\frac{1}{z} - 1 \right) + a_2 \pi \alpha_s(m)(1-z) + a_3 \pi \alpha_s(m)\ln(z) + a_4 \pi \alpha_s(m)[1 - z^{1 - 13 C_A /(6\beta_0)}]$$

$$+ a_5 \pi \alpha_s(m)[1 - z^{1 - 2 C_A /\beta_0}] + a_6 \pi \alpha_s(m)\left[\frac{\pi^2}{12} - \frac{1}{2}\ln^2(2) - \ln(w)\ln\left(\frac{2w}{2w-1} \right) - \mathrm{Li}_2\left(\frac{1}{2w} \right) \right]$$

$$+ a_7 \pi \alpha_s(m)\left[\frac{w}{2w-1}\ln(w) - \frac{1}{2}\ln(2w-1) \right], \tag{45}$$

where $z = \alpha_s(m\nu)/\alpha_s(m)$ and $w = \alpha_s(m\nu^2)/\alpha_s(m\nu)$. The coefficients a_i in Eq. (45) are

$$a_1 = \frac{32 C_A C_F(C_A + 2 C_F)}{3\beta_0^2},$$

$$a_2 = \frac{-C_F[3\beta_0(26 C_A^2 + 19 C_A C_F - 32 C_F^2) + C_A(208 C_A^2 + 597 C_A C_F + 716 C_F^2)]}{78\beta_0^2 C_A},$$

$$a_3 = \frac{-C_F}{3\beta_0^2(6\beta_0 - 13 C_A)(\beta_0 - 2 C_A)} \{ 2 C_F^2(66\beta_0 - 179 C_A)(\beta_0 - 2 C_A)$$

$$- C_A C_F[6(49 - 3\mathbf{S}^2)\beta_0^2 - (1126 - 39\mathbf{S}^2)\beta_0 C_A + 1067 C_A^2] - 24 C_A^2(6\beta_0 - 13 C_A)(\beta_0 - 2 C_A) \},$$

$$a_4 = \frac{-24 C_F^2(3\beta_0 - 11 C_A)(5 C_A + 8 C_F)}{13 C_A(6\beta_0 - 13 C_A)^2}, \quad a_5 = \frac{C_F^2[(4\mathbf{S}^2 - 3)\beta_0 + (15 - 14\mathbf{S}^2)C_A]}{6(\beta_0 - 2 C_A)^2},$$

$$a_6 = \frac{-16 C_F^2(C_A + 2 C_F)}{3\beta_0^2}, \quad a_7 = \frac{16 C_A C_F(C_A + 2 C_F)}{\beta_0^2}. \tag{46}$$
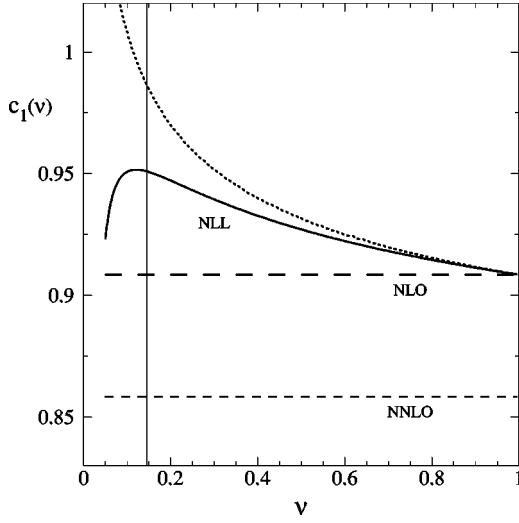
FIG. 7. Values for the $t\bar{t}$ production current coupling $c_1(\nu)$ for $n_f = 5$ massless flavors. At LO and LL $c_1 = 1$. The large and small dashed lines show the value of c_1 at NLO and NNLO [21] respectively. The solid line shows the running value at NLL order given in Eq. (45). The dotted line shows the result of promoting the coupling in the NLO result to a running coupling (the approximation used in Ref. [33]). The solid vertical line marks the Coulombic regime where $\alpha_s(m\nu) = \nu$.

A further check on our result can be made by comparing it to the $\alpha_s^3 \ln^2(\alpha_s)$ corrections calculated by Kniehl and Penin in Ref. [22]. Near threshold the $t\bar{t}$ cross section depends on the product [32]

$$\sigma \propto |c_1|^2 G_C(0,0,E) |\psi_n^C(0)|^2, \tag{47}$$

where ψ^C is the leading order Coulomb wave function, and G_C is the Coulomb Green's function. In the approach used in Ref. [22], G_C embodies corrections to the wave function at the origin, $|\psi(0)|^2 \equiv |\psi_n^C(0)|^2 [1 + \Delta\psi^2(0)]$, and includes the large logarithms. They calculate the $\alpha_s^2 \ln(\alpha_s)$ and $\alpha_s^3 \ln^2(\alpha_s)$ terms and find

$$\Delta\psi^2(0) = -C_F \alpha_s^2 \ln(\alpha_s) \left\{ \left[2 - \frac{2}{3}\mathbf{S}^2 \right] C_F + C_A \right\}$$
$$- \frac{C_F}{\pi} \alpha_s^3 \ln^2(\alpha_s) \left\{ \frac{3}{2}C_F^2 + \left[\frac{41}{12} - \frac{7}{12}\mathbf{S}^2 \right] C_F C_A \right.$$
$$\left. + \frac{2}{3}C_A^2 \right\}, \tag{48}$$

for the terms not involving β_0. In our approach the large logarithms in the cross section all appear in the running coefficient $c_1(\nu)$, so we expect that the logarithms of Kniehl and Penin will be reproduced by

$$\Delta\psi^2(0) = \left| \frac{c_1(\nu)}{c_1(1)} \right|^2 - 1 = 2\ln(\alpha_s)\gamma_{c_1}(1) + \ln^2(\alpha_s)\{\gamma'_{c_1}(1)$$
$$+ 2[\gamma_{c_1}(1)]^2\} + \cdots, \tag{49}$$

where we have expanded to second order in $\ln(\nu) = \ln(\alpha_s)$. The $[\gamma_{c_1}(1)]^2$ term does not contribute at order $\alpha_s^3 \ln^2 \alpha_s$, and can be dropped. The remaining terms in Eq. (49) give

$$\Delta\psi^2(0) = -C_F \alpha_s^2 \ln(\alpha_s) \left\{ \left[2 - \frac{2}{3}\mathbf{S}^2 \right] C_F + C_A \right\}$$
$$- \frac{C_F}{\pi} \alpha_s^3 \ln^2(\alpha_s) \left\{ \frac{3}{2}C_F^2 + \left[\frac{41}{12} - \frac{7}{12}\mathbf{S}^2 \right] C_F C_A \right.$$
$$\left. + \frac{2}{3}C_A^2 - \frac{\beta_0}{2} \left[\left(2 - \frac{2}{3}\mathbf{S}^2 \right) C_F + C_A \right] \right\}, \tag{50}$$

which agrees exactly with the result from Ref. [22] in Eq. (48) after setting $\beta_0 = 0$. Thus, we have shown that the logarithms of Kniehl and Penin can indeed be associated with renormalization group logarithms. Expanding Eq. (45) to higher orders gives the $\alpha_s^4 \ln^3(\alpha_s), \alpha_s^5 \ln^4(\alpha_s)$, etc. terms.

For QCD with $n_f = 5$, the coefficients in Eq. (46) are

$$a_1 = 4.113, \quad a_2 = -2.173, \quad a_3 = 4.308 - 0.417\mathbf{S}^2,$$

$$a_4 = 5.731,$$

$$a_5 = 2.347 - 1.209\mathbf{S}^2, \quad a_6 = -0.914, \quad a_7 = 6.170. \tag{51}$$

The running coefficient $c_1(\nu)$ is shown in Fig. 7 for $\mathbf{S}^2 = 2$. For comparison we have also shown by a dotted line the value of the running coefficient obtained in Ref. [33] by an approach based on simply taking $\alpha_s \to \alpha_s(m\nu)$ to approximate the NLL value for the coupling. This approximation misses many of the $\alpha_s \ln(\nu)$ terms, and does not provide a good estimate of the NLL result, as seen in Fig. 7. Some of the more important logarithms in our NLL result include the large $\ln(m\nu^2/m)$ terms that enter through the mixing generated by ultrasoft gluon diagrams in the potential.

We have also shown the NNLO value for c_1 in Fig. 7. As pointed out in Ref. [21] the NNLO value of $c_1(1)$ is fairly large. From Fig. 7 we see that summing the logarithms reduced the size of the NLO matching correction by a factor of two. It would be interesting to see if the running induced at NNLL continues to improve the convergence of the expansion. A consistent calculation at this order requires the three-loop anomalous dimension of c_1, as well as one loop running of the v^2 coefficients c_2 and c_3. This computation appears quite involved since running of the current at this order will likely depend on the running of higher order terms in the potential.

Several groups have analyzed the $t\bar{t}$ cross section predictions at NNLO using effective field theory techniques [33–37,31]. It should be straightforward to incorporate the renormalization group improved current and potentials into their analysis by simply choosing a value of ν appropriate to the threshold region. The value of ν only needs to be of order the velocities in this region for the large logarithms to be mini-

mized. Additional logarithms that appear in evaluating matrix elements with the potential will not involve large ratios of scales since they are of the form $\ln(E/\mu_U)$ and $\ln(|\mathbf{k}|/\mu_S)$ where $\mu_U = mv^2$ and $\mu_S = mv$. In a more precise analysis one might wish to use $\alpha_s(mv)C_F = v$ to determine the value v to use.

ACKNOWLEDGMENTS

APPENDIX A: LL VALUES FOR THE ORDER v^{-2} AND v^0 POTENTIALS

The leading log values for the coefficients of the $V^{(-2)}$ and $V^{(0)}$ potentials are [19]

$$\mathcal{V}_c^{(T)}(\nu) = 4\pi\alpha_s(m)z,$$

$$\mathcal{V}_c^{(1)}(\nu) = 0,$$

$$\mathcal{V}_r^{(T)}(\nu) = 4\pi\alpha_s(m)z - \frac{32\pi C_A}{3\beta_0}\alpha_s(m)[1-z] - \frac{64\pi C_A}{3\beta_0}\alpha_s(m)\ln(w),$$

$$\mathcal{V}_2^{(T)}(\nu) = \frac{\pi[C_A(352C_F + 91C_d - 144C_A) - 3\beta_0(33C_A + 32C_F)]}{39\beta_0 C_A}\alpha_s(m)[z-1]$$

$$+ \frac{8\pi(3\beta_0 - 11C_A)(5C_A + 8C_F)\alpha_s(m)}{13C_A(6\beta_0 - 13C_A)}[z^{(1-13C_A/(6\beta_0))} - 1]$$

$$+ \frac{\pi(\beta_0 - 5C_A)\alpha_s(m)}{(\beta_0 - 2C_A)}[z^{(1-2C_A/\beta_0)} - 1] - \frac{8\pi(4C_F + C_d - 3C_A)}{3\beta_0}\alpha_s(m)\ln(w),$$

$$\mathcal{V}_2^{(1)}(\nu) = \frac{28\pi C_1}{3\beta_0}\alpha_s(m)(1-z) + \frac{32\pi C_1}{3\beta_0}\alpha_s(m)\ln(w),$$

$$\mathcal{V}_s^{(T)}(\nu) = \frac{2\pi\alpha_s(m)}{(2C_A - \beta_0)}\left[C_A + \frac{1}{3}(2\beta_0 - 7C_A)z^{(1-2C_A/\beta_0)}\right] + \frac{1}{N_c}\pi\alpha_s(m),$$

$$\mathcal{V}_s^{(1)}(\nu) = \frac{(N_c^2 - 1)}{2N_c^2}\pi\alpha_s(m),$$

$$\mathcal{V}_t^{(T)}(\nu) = -\frac{\pi\alpha_s(m)}{3}z^{(1-2C_A/\beta_0)},$$

$$\mathcal{V}_\Lambda^{(T)}(\nu) = 2\pi\alpha_s(m)[z - 4z^{(1-C_A/\beta_0)}], \tag{A1}$$

where $z = \alpha_s(m\nu)/\alpha(m), w = \alpha_s(m\nu^2)/\alpha(m\nu)$, and we have included the N_c dependent terms that come from matching the tree level annihilation diagrams. In the color singlet channel, $\mathcal{V}_t(\nu)$ and $\mathcal{V}_\Lambda(\nu)$ were first calculated in Ref. [18] and agree with Eq. (A1).

APPENDIX B: POTENTIAL OPERATORS THAT VANISH ON-SHELL

It is interesting to consider how the soft and ultrasoft anomalous dimensions for $V^{(-1)}$ are affected when operators

that vanish on-shell are included in the potential Lagrangian, $\mathcal{L}_p$. These new operators can have nontrivial anomalous dimensions. In this Appendix we consider two examples of how including these operators affects intermediate results, but in the end yield the same result as the on-shell potential for observables. Equivalently, it is shown that running the Lagrangian with the new operators from $\nu=1$ to $\nu=v$ and then removing them by field redefinitions or operator identities reproduces the on-shell running value of $V^{(-1)}$.

Consider the scattering $Q(p_1^0,\mathbf{p})+\bar{Q}(p_2^0,-\mathbf{p}) \rightarrow Q(p_3^0,\mathbf{p}')+\bar{Q}(p_4^0,-\mathbf{p}')$. As our first example, consider including in the v^0 potential in Eq. (10) terms of the form:

$$V^{(0)}=[\mathcal{V}_{\Delta 1}^{(T)}(T^A\otimes\bar{T}^A)+\mathcal{V}_{\Delta 1}^{(1)}(1\otimes 1)]\frac{(p_3^0-p_1^0)^2}{\mathbf{k}^4}$$
$$+[\mathcal{V}_{\Delta 2}^{(T)}(T^A\otimes\bar{T}^A)+\mathcal{V}_{\Delta 2}^{(1)}(1\otimes 1)]\frac{(\mathbf{p}'^2-\mathbf{p}^2)^2}{4m^2\mathbf{k}^4}.$$
(B1)

We will refer to this potential as an off-shell potential, since on-shell it vanishes by energy conservation, where $p_3^0=p_1^0,\mathbf{p}'^2=\mathbf{p}^2$. Define $V_\Delta^{(T,1)}=V_{\Delta 1}^{(T,1)}+V_{\Delta 2}^{(T,1)}$. In Ref. [23] it was shown that there is an operator identity whereby the time ordered product of a $\mathcal{V}_c$ and a $\mathcal{V}_\Delta$ potential gives $\mathcal{V}_k$ potentials:

$$+\ \ =\ \frac{i\mathcal{V}_c^{(T)}\mathcal{V}_\Delta^{(T)}}{32mk}\,T^AT^B\otimes\bar{T}^A\bar{T}^B+\frac{i\mathcal{V}_c^{(T)}\mathcal{V}_\Delta^{(1)}}{32mk}\,T^A\otimes\bar{T}^A+\dots,$$
(B2)

where the ellipses denote additional terms which vanish on-shell. The identity in Eq. (B2) allows us to remove the potential in Eq. (B1) at an arbitrary velocity scale ν in favor of a purely on-shell potential. Transforming $\mathcal{V}_\Delta^{(T,1)}(\nu)\rightarrow 0$ gives

$$\mathcal{V}_k^{(T)}(\nu)\rightarrow\mathcal{V}_k^{(T)}(\nu)+\frac{1}{32\pi^2}\mathcal{V}_c^{(T)}(\nu)$$
$$\times\left[-\mathcal{V}_\Delta^{(1)}(\nu)+\frac{1}{4}(C_A+C_d)\mathcal{V}_\Delta^{(T)}(\nu)\right],$$

$$\mathcal{V}_k^{(1)}(\nu)\rightarrow\mathcal{V}_k^{(1)}(\nu)-\frac{1}{32\pi^2}\mathcal{V}_c^{(T)}(\nu)C_1\mathcal{V}_\Delta^{(T)}(\nu).$$
(B3)

In a situation where $\mathcal{V}_\Delta^{(1)}(\nu)=0$ transforming $\mathcal{V}_\Delta^{(T)}(\nu)\rightarrow 0$ induces a color singlet $1/|\mathbf{k}|$ potential of the form

$$\mathcal{V}_k^{(s)}(\nu)\rightarrow\mathcal{V}_k^{(s)}(\nu)-\frac{C_F^2}{32\pi^2}\mathcal{V}_c^{(T)}(\nu)\mathcal{V}_\Delta^{(T)}(\nu).$$
(B4)

(Transformations between order $1/v$ and v^0 potentials were also considered in Refs. [32,35,38].)

To make the implications of Eq. (B3) more clear, we will consider an example and show that including the $V_\Delta^{(T,1)}$ potential will not effect predictions for observables when running below m. Consider matching offshell in Feynman gauge where the matching coefficients at $\nu=1$ are $V_\Delta^{(T)}=4\pi\alpha_s(m)$ and $V_\Delta^{(1)}=0$, and the one loop anomalous dimensions for the potentials in Eq. (B1) are [23]

$$\nu\frac{\partial}{\partial\nu}\mathcal{V}_\Delta^{(T)}=-2\beta_0\alpha_s(m\nu)^2,$$

$$\nu\frac{\partial}{\partial\nu}\mathcal{V}_\Delta^{(1)}=0.$$
(B5)

This anomalous dimension has contributions from the one loop graphs with two soft gluons, ghosts or quarks where:

the two factors of $(\mathbf{p}'^2-\mathbf{p}^2)$ are from the soft vertices, or these factors are from two insertions on the soft propagators, or where one factor is from the propagator and one from the vertex (for the ghost loop). The solution of Eq. (B5) is $V_\Delta^{(T)}(\nu)=4\pi\alpha_s(m\nu)$ and $V_\Delta^{(1)}(\nu)=0$. The one loop counterterm which generates this running affects our soft anomalous dimension computation since now there are counterterms of the form

$$\frac{(\mathbf{p}'^2-\mathbf{p}^2)^2}{m^2(\mathbf{p}'-\mathbf{p})^4\epsilon}.$$
(B6)

These counterterms give rise to one loop diagrams which exactly cancel the divergences in Eq. (26) for the two loop graph in Fig. 3(a). Recalling that the one loop matching values for the $1/|\mathbf{k}|$ potentials are also different [23], we find that the running $\mathcal{V}_k^{(T,1)}(\nu)$ coefficients in Eq. (33) become

$$\mathcal{V}_k^{(T)}(\nu)=\frac{(3C_A-C_d)}{4}\alpha_s^2(m)+\left[\frac{(3C_A-C_d)}{4}\right.$$
$$\left.+\frac{8C_A(C_A+C_d)}{3\beta_0}\right](z^2-1)\alpha_s^2(m)$$
$$+\frac{8C_A(C_A+C_d)}{\beta_0}[z-1-2\ln(w)]\alpha_s^2(m),$$
(B7)

$$\mathcal{V}_k^{(1)}(\nu)=C_1\alpha_s^2(m)+\left[C_1-\frac{16C_AC_1}{\beta_0}\right](z^2-1)\alpha_s^2(m)$$
$$-\frac{48C_AC_1}{\beta_0}\alpha_s^2(m)[z-1-2\ln(w)].$$

This Feynman gauge off-shell potential is consistent with the transformation in Eq. (B3) which transforms the off-shell case, $V_\Delta^{(T)}=4\pi\alpha_s(m\nu)$ and Eq. (B7), into the on-shell case,

$V_\Delta^{(T,1)} = 0$ and Eq. (33). The comparison in Sec. IV A with Ref. [15] shows that our on-shell analysis is also consistent with an off-shell Coulomb gauge potential.

With the off-shell potential in Eq. (B1) there are two new graphs which contribute to the anomalous dimension for the production current:

(B8)

and the anomalous dimension is therefore

$$\nu \frac{\partial}{\partial \nu} \ln[c_1(\nu)] = \frac{-\mathcal{V}_c^{(s)}(\nu)}{16\pi^2} \left(\frac{\mathcal{V}_c^{(s)}(\nu)}{4} + \mathcal{V}_2^{(s)}(\nu) + \mathcal{V}_r^{(s)}(\nu) \right.$$
$$\left. + \mathbf{S}^2 \mathcal{V}_s^{(s)}(\nu) \right) + \frac{\mathcal{V}_k^{(s)}(\nu)}{2} - \frac{\mathcal{V}_c^{(s)} \mathcal{V}_\Delta^{(s)}}{64\pi^2},$$

(B9)

where $\mathcal{V}_\Delta^{(s)}(\nu) = \mathcal{V}_\Delta^{(1)}(\nu) - C_F \mathcal{V}_\Delta^{(T)}(\nu)$. Since the last two terms in Eq. (B9) are invariant under the transformation in Eq. (B4) the off-shell potential gives the same prediction for the running of the production current. In calculating observables the operator identity in Eq. (B2) guarantees that the time ordered product of the running $\mathcal{V}_\Delta^{(T)}$ and $\mathcal{V}_c^{(T)}$ produces the same effect as the soft contribution to the running of the on-shell $\mathcal{V}_k^{(T)}$ in Eq. (26).

As our second example, consider including an operator which would vanish by the lowest order free equations of motion:

$$\mathcal{L}_{eom} = -\sum_{\mathbf{p},\mathbf{p}'} \frac{\mathcal{V}_F}{(\mathbf{p}'-\mathbf{p})^2} \left[\psi_{\mathbf{p}'}^\dagger T^A \left(i\partial_0 - \frac{\mathbf{p}^2}{2m} \right) \psi_\mathbf{p} \right] \chi_{-\mathbf{p}'}^\dagger \bar{T}^A \chi_{-\mathbf{p}}$$
$$+ \chi \leftrightarrow \psi.$$

(B10)

The only feature of the operator in Eq. (B10) that is different from typical operators that vanish by the equations of motion (for example, in HQET [27]) is its nonlocal nature relative to the scales $\mathbf{p} \sim \mathbf{p}' \sim m\upsilon$. At one loop there are ultrasoft gluon graphs which mix into the operator in Eq. (B10), for instance from the diagrams

(B11)

In the first graph the vertex is the first term in Eq. (16) and

the ultrasoft gluon is $\mathbf{A}$, while in the second diagram the cross is an insertion of the ultrasoft ∇^2/m operator in Eq. (7) and the gluon is an A^0. In Feynman gauge both graphs produce a divergence of the form

$$\frac{(E - \mathbf{p}^2/m)}{\epsilon(\mathbf{p}'-\mathbf{p})^2},$$

(B12)

which vanishes by the equations of motion, but off-shell renormalizes the coefficient of the operator in Eq. (B10). To see how this effects the calculation of our ultrasoft anomalous dimension, consider Coulomb gauge, where only Eq. (B11a) is nonzero. In this case there is a one loop counterterm diagram which exactly cancels the divergence in Eq. (28b). After running down to the low scale the value of $\mathcal{V}_k^{(T,1)}(\nu)$ is different, but our potential also includes the operator in Eq. (B10) with coefficient $\mathcal{V}_F(\nu)$. If we wish to remove the operator in Eq. (B10) we can do so with a field redefinition

$$\psi_\mathbf{p}^\dagger \to \psi_\mathbf{p}^\dagger + \sum_{\mathbf{p}''} \frac{\mathcal{V}_F}{(\mathbf{p}'-\mathbf{p})^2} \psi_{\mathbf{p}''}^\dagger T^A \chi_{-\mathbf{p}''}^\dagger \bar{T}^A \chi_{-\mathbf{p}}, \quad (B13)$$

which induces a term from the $\psi_\mathbf{p}^\dagger[i\partial_0 - \mathbf{p}^2/(2m)]\psi_\mathbf{p}$ Lagrangian which cancels Eq. (B10). This field redefinition also gives other new contributions. For us the important point is that the Coulomb potential induces a six-quark operator of the form

$$-\sum_{\mathbf{p},\mathbf{p}'} \sum_{\mathbf{p}''} \psi_{\mathbf{p}''}^\dagger \chi_{-\mathbf{p}''}^\dagger \chi_{-\mathbf{p}'} \psi_\mathbf{p} \chi_{-\mathbf{p}'}^\dagger \chi_{-\mathbf{p}} \frac{\mathcal{V}_F \mathcal{V}_c}{(\mathbf{p}''-\mathbf{p}')^2(\mathbf{p}'-\mathbf{p})^2}.$$

(B14)

(The contraction of color indices and factors of T^A have been suppressed.) Usually a six quark operator could not possibly effect the running of a four quark operator such as the $1/|\mathbf{k}|$ potential. However, because of the momentum dependence in the denominator of Eq. (B14) it induces a nonzero tadpole diagram where the fields $\chi_{-\mathbf{p}'}$ and $\chi_{-\mathbf{p}'}^\dagger$ are contracted. This tadpole graph produces a $1/|\mathbf{k}|$ and makes up for the running in $\mathcal{V}_k$ that was removed when the contribution from Eq. (28b) was canceled by a $\mathcal{V}_F$ counterterm.

[1] W. E. Caswell and G. P. Lepage, Phys. Lett. **167B**, 437 (1986).

[2] G. T. Bodwin, E. Braaten, and G. P. Lepage, Phys. Rev. D **51**, 1125 (1995); **55**, 5853(E) (1997).

[3] P. Labelle, Phys. Rev. D **58**, 093013 (1998).

[4] M. Luke and A. V. Manohar, Phys. Rev. D **55**, 4129 (1997).

[5] A. V. Manohar, Phys. Rev. D **56**, 230 (1997).

[6] B. Grinstein and I. Z. Rothstein, Phys. Rev. D **57**, 78 (1998).

[7] M. Luke and M. J. Savage, Phys. Rev. D **57**, 413 (1998).

[8] A. Pineda and J. Soto, Nucl. Phys. B (Proc. Suppl.) **64**, 428 (1998).

[9] A. Pineda and J. Soto, Phys. Rev. D **58**, 114011 (1998).

[10] M. Beneke and V. A. Smirnov, Nucl. Phys. **B522**, 321 (1998).

[11] H. W. Griesshammer, Phys. Rev. D **58**, 094027 (1998).

[12] A. Pineda and J. Soto, Phys. Rev. D **59**, 016005 (1999).

[13] B. A. Kniehl and A. A. Penin, Nucl. Phys. **B563**, 200 (1999).

[14] M. E. Luke, A. V. Manohar, and I. Z. Rothstein, Phys. Rev. D **61**, 074025 (2000).

[15] N. Brambilla, A. Pineda, J. Soto, and A. Vairo, Phys. Lett. B **470**, 215 (1999); Nucl. Phys. **B566**, 275 (2000).

[16] M. Peter, Phys. Rev. Lett. **78**, 602 (1997); Y. Schröder, Phys. Lett. B **447**, 321 (1999).

[17] N. Brambilla, A. Pineda, J. Soto, and A. Vairo, Phys. Rev. D **60**, 091502 (1999).

[18] Y.-Q. Chen, Y.-P. Kuang, and R. J. Oakes, Phys. Rev. D **52**, 264 (1995).

[19] A. V. Manohar and I. W. Stewart, Phys. Rev. D **62**, 014033 (2000).

[20] A. H. Hoang, Phys. Rev. D **56**, 5851 (1997); **56**, 7276 (1997).

[21] A. Czarnecki and K. Melnikov, Phys. Rev. Lett. **80**, 2531 (1998); M. Beneke, A. Signer, and V. A. Smirnov, *ibid.* **80**, 2535 (1998).

[22] B. A. Kniehl and A. A. Penin, Nucl. Phys. **B577**, 197 (2000).

[23] A. V. Manohar and I. W. Stewart, Phys. Rev. D **62**, 074015 (2000).

[24] M. Luke and A. V. Manohar, Phys. Lett. B **286**, 348 (1992).

[25] S. N. Gupta and S. F. Radford, Phys. Rev. D **24**, 2309 (1981).

[26] S. Titard and F. J. Yndurain, Phys. Rev. D **49**, 6007 (1994).

[27] E. Eichten and B. Hill, Phys. Lett. B **243**, 427 (1990); A. Falk, B. Grinstein, and M. Luke, Nucl. Phys. **B357**, 185 (1991); B. Blok, J. Körner, D. Pirjol, and J. Rojas, *ibid.* **B496**, 358 (1997); C. Bauer and A. Manohar, Phys. Rev. D **57**, 337 (1998).

[28] S. Coleman and R. Norton, Nuovo Cimento **38**, 5018 (1965).

[29] T. Mehen and I. W. Stewart, Nucl. Phys. **A665**, 164 (2000).

[30] J. C. Collins, *Renormalization* (Cambridge University Press, Cambridge, England, 1984).

[31] A. A. Penin and A. A. Pivovarov, Nucl. Phys. **B550**, 375 (1999).

[32] A. H. Hoang, Phys. Rev. D **59**, 014039 (1999).

[33] M. Beneke, A. Signer, and V. A. Smirnov, Phys. Lett. B **454**, 137 (1999).

[34] A. H. Hoang and T. Teubner, Phys. Rev. D **58**, 114023 (1998); **60**, 114027 (1999).

[35] K. Melnikov and A. Yelkhovsky, Nucl. Phys. **B528**, 59 (1998).

[36] O. Yakovlev, Phys. Lett. B **457**, 170 (1999).

[37] T. Nagano, A. Ota, and Y. Sumino, Phys. Rev. D **60**, 114014 (1999).

[38] N. Brambilla, A. Pineda, J. Soto, and A. Vairo, Phys. Rev. D **63**, 014023 (2001).